Surface-Enhanced Raman Spectroscopic Study of 1,4-Phenylene Diisocyanide Adsorbed on Gold and Platinum-Group Transition Metal Electrodes

Scott M. Gruenbaum, Matthew H. Henney, Sachin Kumar, and Shouzhong Zou*

Department of Chemistry and Biochemistry, Miami University, Oxford, Ohio 45056

Received: December 19, 2005; In Final Form: January 19, 2006

Self-assembled monolayers of 1, 4-phenylene diisocyanide (PDI) were formed on Au and Pt-group transition metals and examined by surface-enhanced Raman spectroscopy under controlled applied potential. On all of the metals examined, PDI adsorbs in an edge-on manner, with one NC group bound to the surface and the other pointing away from the surface. The N−C stretching frequency (ν_{NC}) suggests that depending on the metal, PDI adsorbs on different binding sites: terminal sites on Au, both terminal and bridging on Rh and Pt, and predominantly 3-fold hollow sites for Pd. This binding site preference can be understood in terms of the difference in d-band center energy and d-orbital filling among the metals. The applied potential affects the N−C bonding differently as inferred from the potential dependence of ν_{NC}. On Au, Rh, and Pd, the ν_{NC} increases linearly with the applied potential, yielding a Stark tuning slope, $d\nu_{NC}/dE$, of 25, 12, and 10 cm^{-1}/V, respectively. On Pt, the ν_{NC} is nearly independent of the applied potential. On all of the metals studied, the frequencies of benzene ring vibration modes are not dependent on the applied potential, consistent with the edge-on orientation in which the ring does not directly interact with the surface. Several ring vibrations are, however, sensitive to the nature of metal substrate due to different binding sites involved. The ability of the free NC group to function as an anchoring point is demonstrated by the attachment of gold nanoparticles on PDI-covered Au and Pd. The study provides useful NC−metal bonding information for isocyanide-based molecular electronic developments.

I. Introduction

Self-assembled monolayers of organic molecules on metal surfaces have attracted much attention in the past two decades, due to their widespread applications including surface property modifications and molecular electronics.[1−5] The monolayers are usually formed by organic thiols.[1−5] Recently, it was shown both theoretically[6] and experimentally[7,8] that isocyanide may be a better candidate for the anchoring group in molecular electronics as compared to the much more extensively studied thiols, because the barrier for electron transport is lower.[6−8] Despite that the isocyanide transition metal complexes are well studied,[9−12] the adsorption of isocyanides on metal surfaces has not been explored in detail.

Earlier studies of isocyanide adsorption almost exclusively focus on methyl isocyanide (MeNC) in ultrahigh vacuum (UHV) with use of electron energy loss spectroscopy (EELS). On Ni-(111), Friend et al. observed a band at 1760 cm^{-1} at low coverages and an additional feature at 2160 cm^{-1} at higher coverages.[13] The higher frequency band was assigned to the N−C stretching mode (ν_{NC}) of solid methyl isocyanide and the lower frequency feature to the N−C stretch of adsorbed MeNC. The ν_{NC} is significantly redshifted as compared to the gas-phase value (2166 cm^{-1}). Two adsorption orientations were proposed: the C end binds to two Ni atoms (bridging site) or both N and C bind to Ni atoms. On Rh(111), two bands were also observed, one located at 1710 cm^{-1} dominant at low coverages, and one at 2170 cm^{-1} dominant at high coverages.[14] The former was assigned to the ν_{NC} of the bridging bound MeNC and the latter to that of the atop bound. In contrast, on Pt(111) a band at 2240 to 2265 cm^{-1} was observed at low coverages and a second feature at 1600 to 1770 cm^{-1} appears at higher coverages.[15] The higher frequency band is attributed to the ν_{NC} from terminally bonded MeNC and the lower one to 2-fold bridging bound species. This observation was confirmed more recently by Kang and Trenary using infrared reflection−absorption spectroscopy (IRAS).[16] Methyl isocyanide adsorption on Pd(111) was also examined recently by Murphy et al. in UHV using IRAS.[17] At low coverages, both N and C bound to the surface yielding a ν_{NC} at around 1840 cm^{-1}; at high coverages, a new band appears at 2170 cm^{-1} accompanied by the disappearance of the 1840 cm^{-1} feature, which was attributed to the adsorption orientation change from the NC axis parallel to the surface to the NC axis normal to the surface.

Most of the studies of isocyanide adsorption in ambient environment were done on Au. Angelici and co-workers examined extensively the adsorption of various isocyanides on Au powders.[18−21] A general finding is that isocyanides adsorb on terminal (atop) sites through the carbon atom of the NC group. For diisocyanides, depending on the molecular structure, the adsorption can be through either one or both NC groups.[19] 1,4-Phenylene diisocyanide (PDI) was found to adsorb through one of the NC groups in an end-on fashion with the benzene ring pendant.[20] The IR spectrum shows two bands at 2180 and 2121 cm^{-1}, which were attributed to the ν_{NC} for the bound and free NC groups, respectively.[20] Consistent with this, PDI adsorption on gold films deposited on Si also takes the end-on configuration, as shown by IRAS.[22] In this work, the PDI layer thickness measured by ellipsometry suggested that PDI is oriented vertically on the surface.[22] Similar PDI adsorption orientation was also found on Cu and Ag.[23−25] In addition to

* To whom correspondence should be addressed. Phone: 513-529 8084. Fax: 513-529 5715. E-mail: zous@muohio.edu.

10.1021/jp057393e CCC: $33.50
Published on Web 02/14/2006

IR studies, there are several surface-enhanced Raman spectroscopic (SERS) studies of the adsorption of PDI and related isocyanides on Au nanoparticle aggregates.[26−28] Essentially the same adsorption orientation was concluded. In a recent report, we demonstrated that ν_{NC} blueshifts when a layer of Au or Al was evaporated on top of a PDI monolayer on Au, which was attributed to the bonding between originally free NC and the top metal layer, supporting that PDI adsorbs vertically on Au.[29]

The adsorption of isocyanide on Pt-group transition metals is less studied. Hickman et al. showed isocyanides selectively adsorb on Pt over Au.[30,31] Lin and McCarley found that 1,6-diisocyanohexane interacts with Au and Pt mainly with one NC group bound to the surface, and surface polymerization was suggested by the presence of imine bands in the IR spectra.[32] However, no spectrum was shown for Pt. Horswell et al. found that dodecyl isocyanide is terminally bound to Pt nanoparticles as suggested by a ν_{NC} at 2218 cm^{-1}, upshifted from 2147 cm^{-1} of the free molecule.[33] More recently, isocyanide adsorption on Pd was studied with surface IR spectroscopy by several groups. Murphy et al. reported a comparative study of the adsorption of aryl isocyanides, including PDI, on evaporated Pd and Au films.[34] For PDI on Pd, three bands associated with ν_{NC} were observed at 2170, 2120, and 1960 cm^{-1}. These were assigned to ν_{NC} of the σ-bonded (terminal-bound), free, and σ/π-bonded PDI, respectively. Swanson et al. studied the adsorption of PDI and other aryl diisocyanides with up to three benzene rings between the NC groups on evaporated thin Pd and Au films.[35] Two features assignable to ν_{NC} were observed in the PDI IR spectra, one narrower at 2121 cm^{-1} attributed to the ν_{NC} of the free NC group, and the other much broader at 1980 cm^{-1} assigned to the N−C stretch of the PDI bound to 3-fold hollow sites (NC bound to three Pd atoms). In a study of oligo(phenylene-ethynylene) isocyanide adsorption on Pd and Au surfaces, Stapleton et al. also showed an IR band at around 1970 cm^{-1} on Pd, which was assigned to the ν_{NC} of bridging bound isocyanide.[36] In contrast, Pranger and Tannenbaum did not observe any N−C stretching band in their IR study of PDI adsorption on Pt, which they attributed to the flat adsorption of PDI.[23]

Herein we present results from the surface-enhanced Raman spectroscopic study of 1, 4-phenylene diisocyanide adsorption on Au and Pt-group transition metals, including Rh, Pt, and Pd, in electrochemical environment, aiming at examining the effects of metal substrate on the PDI adsorption. One advantage of the electrochemical interface over the solid−air interface is that the surface potential is controlled and variable, facilitating the examination of the influence of surface potential on adsorbate−substrate interaction. This may be a better model system for molecular electronics in which molecules are often subjected to a strong electric field. Compared to surface infrared spectroscopy used in most of the studies of isocyanide adsorption, SERS does not require the background spectral subtraction and covers a wider frequency region.[37,38]

Of particular interest in this paper is to systematically examine the metal dependence of diisocyanide adsorption. On all of the metals examined, PDI adsorbs in an edge-on fashion with one NC group bound to the surface and the other pointing away from the surface. From the ν_{NC} frequency, it is suggested that depending on the nature of the substrate, the diisocyanide adsorbs on different binding sites. On Au, PDI exclusively binds to terminal sites, and on Rh and Pt, both terminal and bridging sites are occupied. The PDI binding on Pd is nearly exclusively on 3-fold hollow sites. This binding site preference is explained in terms of the metal d-band center position. The applied potential affects the N−C bonding differently as inferred from the potential dependence of ν_{NC}. In the potential range examined, on Au, Rh, and Pd, the ν_{NC} increases linearly with the applied potential, while on Pt, the ν_{NC} is nearly independent of the potential. The benzene ring vibrations do not vary with the applied potential, consistent with the edge-on orientation in which the ring does not directly interact with the surface. However, several ring modes are sensitive to the nature of metal substrate. The study provides some insights into the PDI adsorption on metal surfaces and would facilitate the molecular electronic developments with isocyanides.

II. Experimental Section

1. Chemicals. 1,4-Phenylene diisocyanide (PDI, 99%), K_2PtCl_4 (99.99%), $RhCl_3$ (99.9+%), $PdCl_2$ (99.999%), $HAuCl_4 \cdot 3H_2O$ (99.9%), and $CuSO_4 \cdot 5H_2O$ (99.995%) were obtained from Sigma-Aldrich (St. Louis, MO). Semiconductor grade (99.997%) carbon monoxide was from Spectra Gas (Branchburg, NJ). $HClO_4$ (0.1 M) was diluted from concentrated $HClO_4$ (70%, double distilled, GFS, Powell, OH). Absolute ethanol was purchased from Pharmco (Brookfield, CT). All of the chemicals were used as received and the aqueous solutions were prepared with Milli-Q water from a Millipore water purification system (Milli-QA10, Millipore, Bedford, MA).

2. Gold Nanoparticle Fabrication. All glassware used for Au colloid preparations were thoroughly cleaned in aqua regia (3:1 v/v concentrated HCl and HNO_3), rinsed with Milli-Q water, and soaked in water for 1 h prior to use. The colloidal solution of 3, 12, 30, and 60 nm Au particles was prepared according to the reported methods.[39,40] The 30 and 60 nm Au particle solutions were freshly prepared because the particles tend to aggregate in 2 to 3 days.

3. Atomic Force Microscopic Measurements. Atomic force microscopic images were taken with a Pico Plus scanning probe microscope from Molecular Imaging (Tempe, AZ). The images were obtained by using silicon nitride cantilevers with a typical resonance frequency of about 300 kHz in acoustic AC mode (noncontact mode). The substrates employed Au films (150 nm) thermally evaporated onto precleaned glass slides with use of a thermal evaporator (CV301, Cooke Vacuum Products, South Norwalk, CT). Before Au evaporation, the glass slides were heated to 350 °C for 6 h and during the evaporation the substrate temperature was kept at 300 °C with a home-built thermal heating plate. The base pressure for deposition is 8×10^{-7} Torr. The deposited Au films were cooled to room temperature before they were exposed to ambient environment. Au films prepared by this procedure have been shown to mainly consist of a large area of flat (111) terraces.[41−43]

4. FTIR Measurements. The infrared spectrum of PDI powder was recorded with a Perkin-Elmer Spectrum One FTIR spectrometer, equipped with a TGS detector and a universal ATR microcrystal.

5. Surface-Enhanced Raman Spectroscopy (SERS) Measurements. To obtain the surface-enhanced Raman effect, a Au electrode (2 mm in diameter, CH Instruments, Austin, TX) was polished successively with 1.0 and 0.3 μm Al_2O_3 powder on a polishing cloth (Buehler, Lake Bluff, IL) and roughened by electrochemical oxidation−reduction cycles in 0.1 M KCl as described by Gao et al.[44] To obtain SERS on platinum-group transition metals, overlayer strategy was used.[45] In this approach, transition metals were deposited on the roughened Au electrode as ultrathin films (a few monolayers) by two different methods.[46−50] Platinum and palladium thin films were electrodeposited on the SERS active Au surface by a redox

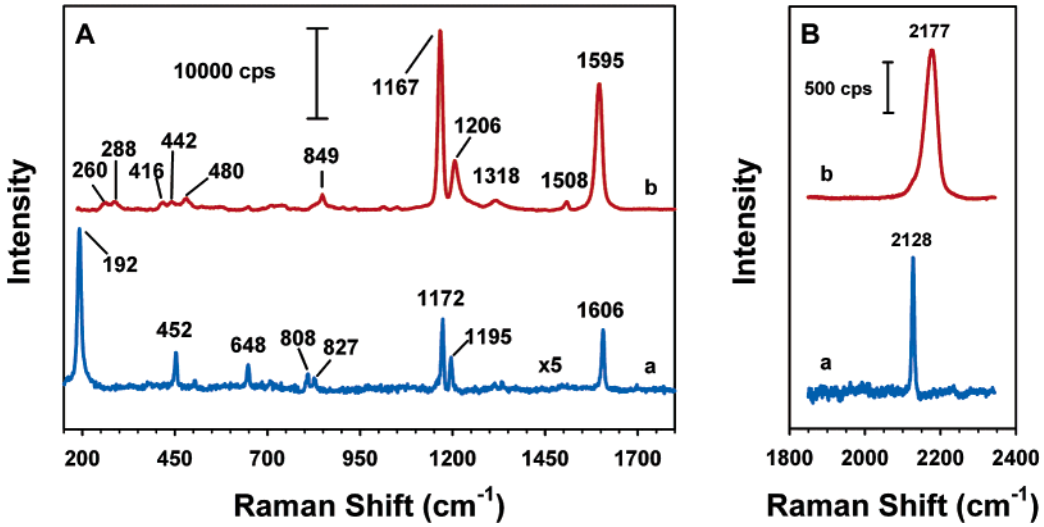

Figure 1. Normal Raman (a) and surface-enhanced Raman (b) spectra in the ring vibration (A) and N−C stretching (B) regions obtained from PDI powder and PDI adsorbed on a Au electrode, respectively. The SER spectrum was recorded in 0.1 M $NaClO_4$ at 0.0 V.

replacement approach.[46−48] To ensure the Au surface is entirely covered by Pt and Pd, 2 to 3 redox replacement cycles (equivalent to 2 to 3 monolayers) were employed. Thicker films yield essentially the same SER features, except that the Raman intensity is weaker, due to the decay of the Raman enhancement effect as the film thickness increases.[45,49] Rhodium films with a nominal thickness of 7 monolayers were prepared by constant current (10 μA, 20 s) deposition from 5 mM $RhCl_3$ + 0.1 M $HClO_4$.[49] The film thickness was estimated from the charge involved in the deposition, assuming hexagonal closed packing of Rh.[49] To form a PDI monolayer, the electrodes were rinsed with absolute ethanol before being immersed in 1 mM PDI ethanol solution overnight (>15 h). The PDI-covered electrodes were then rinsed sequentially with ethanol and water before Raman measurements.

SERS measurements were conducted in a two-compartment, three-electrode glass cell with an optically flat glass as the window at the bottom. A Pt wire was used as the counter electrode and the reference electrode is the Ag/AgCl electrode with saturated KCl (CH Instruments, Austin, TX). The supporting electrolyte is 0.1 M $NaClO_4$ and the electrode potential was controlled by a voltammograph (CV27, BAS, West Lafayette, IN). Raman spectra were collected with a micro-Raman probe (SpectraCode, West Lafayette, IN) equipped with a SpectraPro 300i monochromator (Acton Research, Acton, MA) and a liquid nitrogen cooled red-intensified back illumination CCD detector (Princeton Instruments, Trenton, NJ). The laser excitation at 785 nm was from a diode laser (Process Instruments, Salt Lake City, UT) coupled to an optical fiber bundle and was focused to a 100 μm spot on the sample with a long working distance 20× microscope objective (NA 0.42). The Raman scattering light was collected with the same objective in a backscattering fashion and sent to a monochromator through a second fiber bundle. The Rayleigh scattering light was rejected by a set of Holographic Notch filters (Kaiser Optical Systems, Ann Arbor, MI). The monochromator is equipped with three grating sets (300, 600, and 1200 g/mm). For the ring vibration region, the 600 g/mm grating was used and the 1200 g/mm grating was employed for the N−C stretching region. The laser power at the sample was typically around 5 mW. The Raman shift axis was calibrated with a neon light. Typical spectrum acquisition time was 30 s for the N−C stretching region and 2 to 10 s for the ring vibration region. However, the spectra were plotted with the intensity converted to electron counts per second (cps) and were subjected to a multipoint baseline correction by using GRAMS AI program (Version 7.01, Thermo Electron Corp., Waltham, MA).

All the measurements were conducted at room temperature (23 ± 1 °C).

III. Results and Discussion

1. PDI Adsorption on Au. Displayed in Figure 1 is a SER spectrum of PDI on Au taken in 0.1 M $NaClO_4$ at 0.0 V together with a normal Raman spectrum for comparison. Identical spectra were obtained at the same potential in 0.1 M $HClO_4$. The spectra cover both the ring vibration and N−C stretching regions. Due to the low sensitivity of the detector in the long wavelength region (Raman shift greater than 2800 cm^{-1}), the C−H stretching modes were not observed and therefore this region of the spectrum was not shown. We start with the N−C stretching region (Figure 1B). The normal Raman spectrum in this region contains a single sharp peak (full width at half-maximum (fwhm) = 7 cm^{-1}) at around 2128 cm^{-1}, which can be assigned to the N−C stretching mode. Upon adsorption on Au, significant changes were observed in the spectrum. The band blueshifts to 2177 cm^{-1} and significantly broadens. The fwhm is now around 35 cm^{-1}. In addition to the main peak, there is a weak shoulder located at around 2130 cm^{-1}. This observation is consistent with previous SERS and surface IR studies, which concluded that PDI adsorbs on Au with one NC group attached to the surface and the other pendant.[20,22,28,29] The higher frequency band has been assigned to the N−C stretch from the NC group anchoring on Au and the lower frequency from the free NC.[20,22,28,29] By comparing the N−C stretching frequency of the Au isocyanide complexes, the NC is believed to bind terminally on Au (i.e., one PDI on a single surface atom).[20,51] Similar results were obtained on roughened silver electrodes.

In agreement with this adsorption configuration, the 2177 cm^{-1} band center frequency depends more strongly on the applied potential than that of the 2130 cm^{-1} shoulder. While this shoulder is buried under the main peak at −0.8 V, it is clearly discernible at +0.4 V, as demonstrated in Figure 2. The potential limits are set by the oxidation of PDI above +0.4 V and the hydrogen evolution below −0.8 V. The bonding of isocyanide to metal is considered to be similar to that of carbon monoxide (CO),[11,12,52] which involves electron donation from

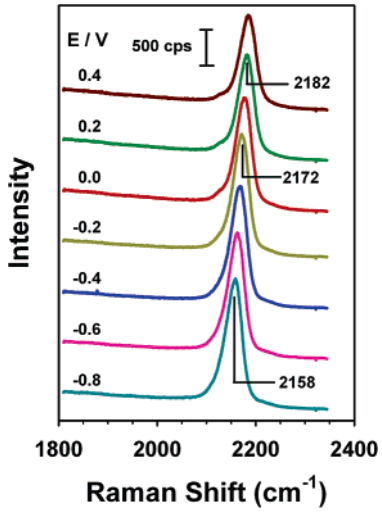

Figure 2. Potential-dependent SER spectra in the N−C stretching region for PDI on Au obtained in 0.1 M $NaClO_4$.

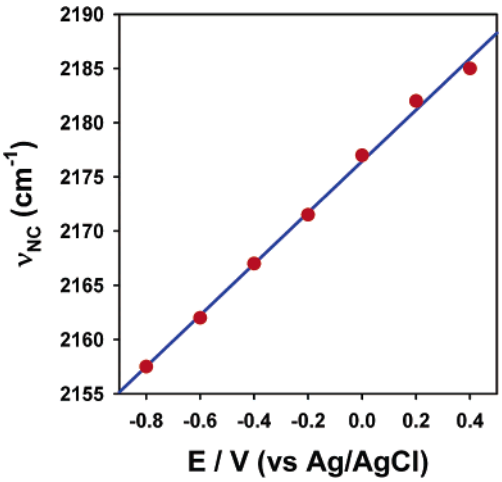

Figure 3. Peak frequency of N−C stretch for PDI adsorbed on Au plotted as a function of applied potential. The data points are taken from the spectra in Figure 2. The solid line serves as a guide to the eye.

the antibonding σ orbital to the metal d-band and π-back-donation from the metal d-band to the π^* antibonding orbital.[52,53] The change of the electrode potential alters the extent of σ-donation and π-back-donation, hence the C−O stretching frequency.[52] In the isocyanide case, the higher ν_{NC} on Au as compared to that of the free molecule is due to the σ-donation from PDI, which strengthens the N−C bond by lowering the electron occupancy of the antibonding orbital. The π-back-donation is less significant. We return to this bonding preference in the Pd section. As the potential became more negative, the σ-donation is weaker and the π-back-donation is stronger, resulting in a weaker N−C bond and a lower N−C stretching frequency (ν_{NC}). At more positive potentials, the opposite occurs. The σ-donation is stronger, yet the π-back-donation is weaker, yielding a higher N−C stretching frequency. This is known as the electrochemical Stark-tuning effect.[54−56] Similar to CO, the ν_{NC} potential dependence is linear, as shown in Figure 3 for the main N−C stretching peak. The Stark tuning slope, $d\nu_{NC}/dE$, for the main peak is around 25 cm^{-1}/V. The $d\nu_{NC}/dE$ cannot be accurately determined for the free NC, but it is definitely smaller than that of the main peak. This is reasonable because the free NC group does not directly interact with the metal surface.[57] Nonetheless, an electrostatic effect from the applied field is apparently present on the free NC, as indicated by the weak potential dependent ν_{NC}. The Stark tuning slope of the bound NC is close to that reported for 1,8-diisocyanooctane adsorbed on Au with use of potential modulated infrared reflection−absorption spectroscopy,[58] albeit the linearity is better in the present case, probably due to the large uncertainty in the NC stretching frequency in the IR spectrum, arising from the spectral subtraction commonly used in the IR studies.

We now switch to the lower frequency region. In the normal Raman spectrum, the most prominent in this region are eight sharp peaks, located at 192, 452, 648, 808, 827, 1172, 1195, and 1606 cm^{-1}. The width for these peaks measured as the full width at half-maximum (fwhm) is no more than 10 cm^{-1}. Several weaker peaks are also discernible in the spectrum. The spectrum is largely the same as that reported in the literature,[28] only with Figure 1 covering a wider frequency region. The assignment of these bands to the normal modes of PDI is listed in Table 1. The band assignment was based on the results from a B3LYP level DFT calculation with the 6-311g basis set.[59] Calculations with other methods or basis sets yield similar results. The calculated values were included in Table 1 together with the IR vibration frequencies obtained from PDI powders (the spectrum is provided in the Supporting Information, Figure S1). The bold values in the calculated results are for the Raman active modes. It is well-known that the vibration frequencies obtained from DFT calculations tend to be larger than the experimental values.[61−63] A common practice is to use frequency correction factors. The values listed in Table 1 were calculated results modified with a correction factor of 0.9659 for frequencies greater than 1800 cm^{-1} and 0.9927 for those below 1800 cm^{-1}.[61] From Table 1, the agreement between the calculated and measured values is excellent, the difference for all but one (192 cm^{-1}) vibration frequency is smaller than 5%. This level of agreement adds confidence in the band assignment.

Upon adsorption to Au, the PDI spectrum changes sharply. In addition to the bands observed in the normal Raman spectrum, many new bands appear. This is typical for SERS and has been attributed to the reduction of molecular symmetry upon adsorption and the field gradient Raman scattering.[64,65] The most prominent of these new bands are located at 260, 288, 416, 480, and 1508 cm^{-1}. A complete list of the observed bands together with their vibration mode assignments are summarized in Table 1. The band assignment largely relies on the assumption that the ring vibration modes only shift slightly upon adsorption. This assumption may not hold for some of the vibration modes, especially when the vibration is strongly coupled to the ν_{NC} of the NC group anchoring on the surface. Therefore most of the band assignments are only tentative. Nevertheless, some of the bands can be confidently assigned based on their relative intensity. For example, the bands at 1167, 1206, and 1595 cm^{-1} can be assigned with high certainty to ν_{9a}, ν_{7a}, and ν_{8a}, respectively. Compared to the normal Raman spectrum, ν_{9a} and ν_{8a} decrease about 5 and 10 cm^{-1}, respectively, whereas ν_{7a} increases more than 10 cm^{-1}. These frequency shifts can be attributed to the changes of PDI intramolecular bonding upon adsorption, caused by the σ-donation and π-back-donation. A more detailed discussion is provided in the Pd section.

The SER frequencies in this spectral region do not depend on the applied potential, as long as the potential is kept in the range shown here. Above +0.4 V, significant spectral changes were observed (Supporting Information, Figure S2), likely from PDI electrooxidation. The relatively narrow bandwidth and the absence of band frequency shift suggest that the aromatic ring does not interact directly with the Au surface, in agreement with the adsorption configuration that only one NC group anchors

TABLE 1: Vibrational Frequencies (cm^{-1}) for Normal Modes of 1,4-phenylene Diisocyanide (PDI) Adsorbed on Metal Surfaces Compared with Corresponding Data from PDI Powder

description[a]	mode[b]/ symmetry[c]	B3LYP/ 6-311 g[d]	Raman[e]	IR[f]	SERS[g]			
					Au	Rh	Pt	Pd
C−NC in-plane bend	β_{NC}, B_{3g}	**178**	192		260		225	216
metal−NC stretch					288			
C−NC out-of-plane bend, in-phase	γ_{NC}, B_{3u}	296			350		334	320
C−C−C in-plane bend	6a, A_g	**394**	381		384	358	380	348
C−C−C out-of-plane bend	16a, A_u	416			416	414	412	414
C−NC out-of-plane bend, out-of-phase	10b, B_{2g}	**439**	452		442	442	436	435
C−NC in-plane bend	15, B_{2u}	441			480	475	478	462
C−NC in-plane bend	9b, B_{3g}	**508**	504		528	530	523	524
C−H out-of-plane bend, in-phase	11, B_{3u}	532			571	552, 603	570	608
C−C−C in-plane bend	6b, B_{3g}	**659**	648		647	647	647	646
C−C−C trigonal bend	12, B_{1u}	672		672	687			683
C−C−C puckering	4, B_{2g}	**727**	709		710	708	707	700
ring breathing	1, A_g	**827**	808		830	825	820	816
C−H out-of-plane bend	10a, B_{1g}	**829**	827		849	844	842	840
C−H out-of-plane bend	17b, B_{3u}	858		845	872	894		868
C−H out-of-plane bend	5, B_{2g}	**964**	903		905	966		964
C−H out-of-plane bend	17a, A_u	962						
C−H in-plane bend	18a, B_{1u}	1029		1028	1012	1005	1014	1014
C−H in-plane bend, out-of-phase	18b, B_{2u}	1124		1106	1050	1075, 1145	1113	1123
C−H in-plane bend	9a, A_g	**1178**	1172		1167	1165	1164	1160
C−NC stretch	13, B_{1u}	1209		1184	1220			
C−NC stretch	7a, A_g	**1218**	1195		1206	1216	1214	1212
C−C stretch, Kekulé	14, B_{2u}	1297		1286	1248	1266?	1230	1237
C−H in-plane bend, in-phase	3, B_{3g}	**1323**	1313		1318	1310	1318	1306
C−C stretch	19b, B_{2u}	1442		1418	1410	1422	1415	1420
C−C stretch	19a, B_{1u}	1525		1502	1508	1502, 1456	1506, 1480	1496
C−C stretch	8b, B_{3g}	**1593**	1590		1595	1562	1564	1549
C−C stretch	8a, A_g	**1634**	1606		1595	1590, 1600	1576, 1592	1588
C−N stretch, asym	ν_{NC}, B_{1u}	2114		2128				
C−N stretch, sym	ν_{NC}, A_g	**2115**	2128		2128, 2177	2165	1912, 2122	1987, 2123
C−H stretch	20a, B_{1u}	3089		3045				
C−H stretch	7b, B_{3g}	**3090**						
C−H stretch	20b, B_{2u}	3101		3094				
C−H stretch, in-phase	2, A_g	**3102**						

[a] Approximate mode description.[60] [b] Wilson notation for normal vibration;[60] [c] Vibration symmetry type for free PDI. [d] Vibration frequencies of free PDI from DFT calculations. The bold values are for Raman active modes. [e] Raman band frequencies for PDI powder obtained in this work. [f] IR band frequencies for PDI powder obtained in this work; [g] SER band frequencies for PDI adsorbed on various metals at 0.0 V in 0.1 M $NaClO_4$ from this work.

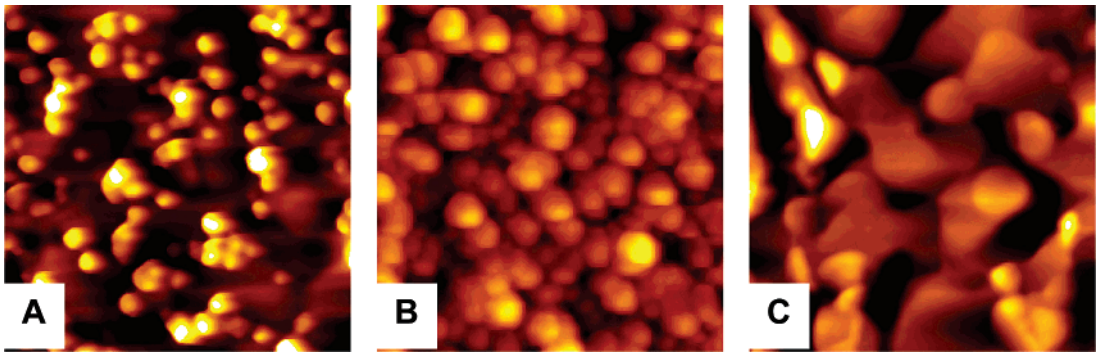

Figure 4. Atomic force microscopic images (1×1 μm^2) of Au thin film (150 nm) coated glass slides with (A and B) and without (C) PDI monolayer after being incubated in a 12 nm Au colloid solution for (A) 10, (B) 60, and (C) 30 min.

on the surface and the other is pendant.[20,22,28,29] Kim et al. reported the SER spectrum for PDI adsorbed on Au nanoparticles, but their spectrum only covers frequencies above 1100 cm^{-1}.[28] In the same frequency region, our results agree well with theirs. Lin and McCarley observed IR bands between 1580 and 1680 cm^{-1}, which signal the oligomerization/polymerization of 1,6-hexane diisocyanide on Au.[32] There is no discernible band between 1600 and 1800 cm^{-1} in the SER spectrum in Figure 1A, indicating the absence of the oligomerization/polymerization. In addition, no spectral changes were observed after the PDI covered Au was immersed in Ni^{2+} solution, which catalyzes isocyanide polymerization,[32] further verifying the absence of polymerization.

To further prove that the PDI interacts with Au through only one NC group, we used Au nanoparticles, with the hypothesis that if the PDI adsorb on Au with only one NC group, the free NC group should function as a "molecular glue" to attach other species, such as nanoparticles, to the PDI-modified surface.[40,66−69] This was indeed observed. Figure 4 displays atomic force microscopic images of Au nanoparticles attached to PDI-modified Au substrates. The images were taken on PDI-coated Au slides soaked in a 12 nm gold particle solution for 10 and

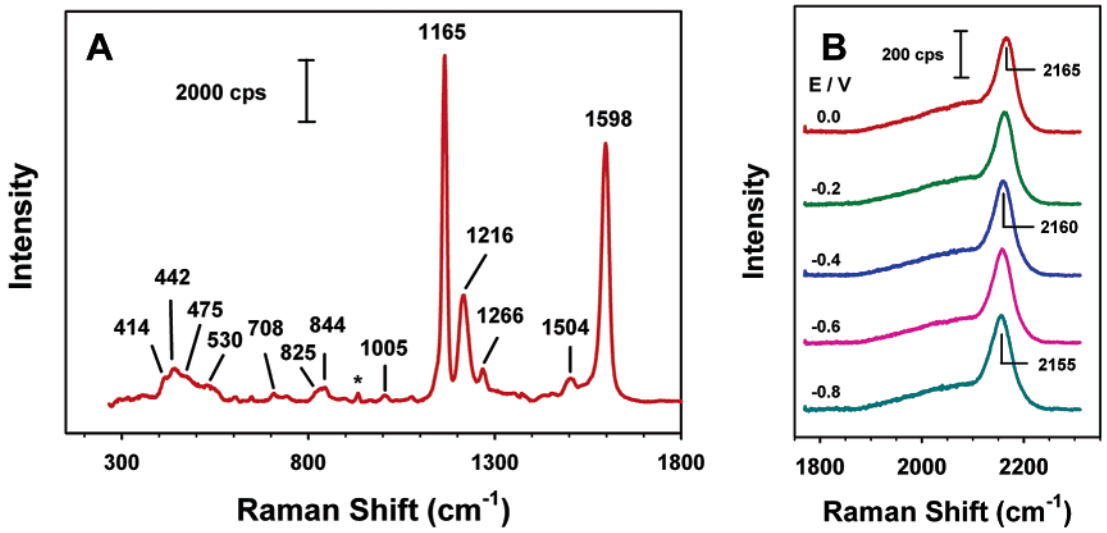

Figure 5. SER spectra obtained on PDI covered Rh electrodes in 0.1 M $NaClO_4$: (A) in the ring vibration region at 0.0 V; (B) in the N−C stretching region at the indicated potentials. The small sharp peak located at 935 cm^{-1} (marked by an asterisk) is from the symmetric stretch of coadsorbed ClO_4^-, which disappears at more negative potentials. A similar but much weaker ClO_4^- band was also observed on other metals.

60 min (Figure 4A,B), respectively. For comparison, an image of a Au slide without a PDI layer incubated in the same Au nanoparticle solution for 30 min was included (Figure 4C). The Au substrates were Au thin films (150 nm) deposited by thermal evaporation on heated glass slides, which yields atomically flat Au terraces.[41−43] The detailed procedure for the gold slide preparation is described in the Experimental Section. From Figure 4, it is clear that with the presence of PDI, Au particles were attached to the surface, and the number of particles as well as the extent of particle aggregation increase with incubation time (Figure 4A,B). Without the PDI layer, there is no particle adsorption (Figure 4C). These experiments confirm that PDI interacts with Au surface through a single NC group, with the benzene ring sticking out of the surface, leaving the second NC group for binding to other species.

2. PDI Adsorption on Rh. Shown in Figure 5 are SER spectra of PDI adsorbed on a Rh electrode, in both ring vibration (A) and NC stretching (B) regions, in 0.1 M $NaClO_4$. Similar to the PDI adsorption on Au, the frequencies for ring vibrational modes do not change with the applied potential within the range examined, therefore only the spectrum taken at 0.0 V was shown. The potential limits are set by the onsets of surface oxidation and hydrogen evolution. We consider first the N−C stretching region. There is a strong peak centered on 2165 cm^{-1} at 0.0 V (Figure 5B). The peak position depends linearly on the applied potential, with a Stark tuning slope of about 12 cm^{-1}/V (Supporting Information, Figure S3). Accompanying this strong peak is a very broad shoulder at the lower frequency side. These features are from PDI adsorbed on Rh. The possibility of the 2165 cm^{-1} band arising from PDI adsorbed on Au pinholes can be ruled out. We examined the uniformity of the Rh film by cycling the applied potential between −0.25 and +1.3 V in 0.1 M $HClO_4$ and no Au oxide reduction peak was observed, indicative of the absence of a significant amount of Au pinholes.[49] The Stark tuning slope observed here is about half of that observed on Au, which provides further evidence that the peak at 2165 cm^{-1} is indeed from PDI adsorbed on Rh.

Compared to the IR spectra of a PDI-linked Rh complex and other Rh complexes with terminally bound isocyanide, which show a strong ν_{NC} between 2140 and 2200 cm^{-1},[70−72] the 2165 cm^{-1} band can be confidently assigned to the N−C stretch from the PDI adsorbed on atop sites. The N−C stretching frequency is higher than that of the free molecule, suggesting that the σ-donation is the main contributor to the NC−Rh bond, similar to the case discussed above for Au. However, the ν_{NC} is lower than that on Au at the same applied potential, suggesting the back-donation is more significantly involved on Rh. This is likely due to the higher d-band center energy of Rh as compared to that of Au, facilitating the back-donation.[52,73,74] The lower frequency shoulder is very broad, covering nearly 200 cm^{-1} from 1900 to 2100 cm^{-1}. This broad feature is probably from isocyanide bound to bridging sites (either 2- or 3-fold sites). The coexistence of the atop and bridging binding is similar to the carbon monoxide adsorption on Rh surfaces.[49]

In the ring vibration region (Figure 5A), the spectrum is dominated by three intense bands located at 1165, 1216, and 1598 cm^{-1}, respectively. Close inspection of these bands reveals that the 1165 and 1598 cm^{-1} features contain one or more shoulders at the lower frequency side. To deconvolute these bands, the peak fitting function in the GRAMS AI program was used. The shoulder next to the 1165 cm^{-1} peak is centered at 1145 cm^{-1}. In addition to the 1504 cm^{-1} peak clearly evident in the spectrum, several other bands can be deconvoluted from the 1598 cm^{-1} feature and they are located at 1422, 1456, 1562, 1590, and 1600 cm^{-1}, respectively. As suggested from the NC stretching mode, both atop and bridging bound PDI are present on Rh. Due to vibration coupling, some of the ring modes are sensitive to the PDI binding site. We tentatively assigned the 1456 and 1502 cm^{-1} features to the ν_{19a} mode, and the 1590 and 1600 cm^{-1} to the ν_{8a} mode of the bridging and atop PDI, respectively. The complete band assignment is listed in Table 1. The rows with two values assigned to a single mode denote that vibration is sensitive to the binding site and the smaller value is assigned to the bridging-bonded PDI. Compared to the spectrum observed on Au, the band positions are largely the same for most of the vibration modes, except for the bands that are sensitive to the binding sites. The relative intensity of some bands is also different on the two surfaces. For the trio at 400 to 500 cm^{-1}, the 442 cm^{-1} band is most intense on Rh, but the 480 cm^{-1} band is the strongest on Au. The bands between 500 and 600 cm^{-1} are significantly more prominent on Rh as compared to Au. These differences may arise from the presence of both atop and bridging bound PDI. The origin of the 1266 cm^{-1} band on Rh is not clear. This band is nearly absent on other metals and sometimes is also much weaker on Rh. We

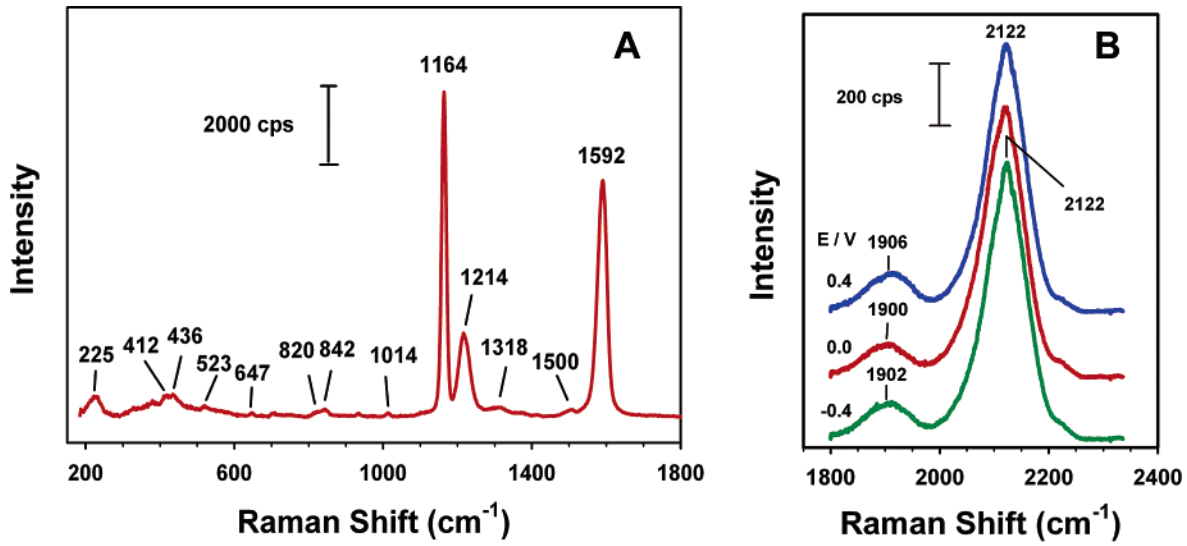

Figure 6. SER spectra obtained on PDI covered Pt electrodes in 0.1 M $NaClO_4$: (A) in the ring vibration region at 0.0 V; (B) in the N−C stretching region at the indicated potentials.

suspect it may be from products of photochemistry, though it is also possibly from ν_{14}. Most of the bands are broadened upon adsorption, presumably due to the coupling between ring and NC vibrations. fwhm is nevertheless smaller than 25 cm^{-1}, which suggests that the ring does not directly interact with the surface, in agreement with the PDI adsorption through a single NC group.

3. PDI Adsorption on Pt. Figure 6 shows SER spectra of PDI adsorption on Pt in 0.1 M $NaClO_4$ in the ring vibration (A) and N−C stretch (B) regions. Similar to the cases on Au and Rh, the ring vibration frequency and intensity do not depend significantly on the applied potential within the examined potential range. A spectrum taken at 0.0 V is therefore shown as a representation. Again we start with the N−C stretching region. Two bands are clearly present, one very strong located at 2122 cm^{-1} and the other much weaker and centered at about 1900 cm^{-1}. The center position for the higher frequency band varies less than 5 cm^{-1} from sample to sample, but that for the lower frequency band fluctuates more significantly (~15 cm^{-1}). The assignment of these two bands is based on the frequency comparison with corresponding inorganic complexes and the analogy with the CO adsorption on Pt.[49,75] The IR spectrum of Pt_3 clusters connected with terminally bound PDI contains a strong band at 2122 cm^{-1},[75] which is at the same position as one of the ν_{NC} observed here. We therefore attribute this band to the atop bound PDI. The assignment of the second band is less straightforward. There is no bridging bound inorganic complex for comparison. By analogy to CO,[49] which has a binding ability very similar to that of the −NC group,[10−12] we tentatively assign this band at around 1900 cm^{-1} to ν_{NC} of PDI bound to two Pt atoms (bridging bound), though 3-fold hollow site binding is also very likely (vide infra). The stretching frequency of the atop bound NC is very close to that of free molecule, suggesting that σ-donation and π-back-donation may contribute equally to the NC−Pt bond. This differs from 1,8-diisocyanooctane adsorbed on Pt nanoparticles, on which a significantly blue-shifted ν_{NC} was observed.[33] On the contrary, the much lower frequency for the bridging bound NC is reminiscent of a much stronger π-back-donation of the bridging binding, typical for CO adsorption on Pt and Rh.[49] This bridging-bound ν_{NC} was not reported on 1,8-diisocyanooctane-coated Pt particles.[33]

Interestingly, unlike the ν_{NC} on Au or Rh, the two bands observed on Pt do not vary linearly with the applied potential and the potential dependence is rather weak, especially for the higher frequency band, of which the center frequency essentially does not change with the applied potential. This may arise from the nearly equal contribution of σ-donation and π-back-donation, on which the applied potential has opposite effects. Both bands are rather broad, with the fwhm being about 100 cm^{-1} for the 1900 cm^{-1} feature and 80 cm^{-1} for the 2122 cm^{-1} feature. The band broadening may result from the inhomogeneity of the surface sites.

A weak peak was always observed at around 2220 cm^{-1}, regardless of how long the Pt surface was incubated in the PDI solution. This is similar to that reported on Pd films,[35] which may come from the impurity produced by surface-enhanced photochemistry.[65] However, this band was not observed on other metal surfaces examined here.

In the ring vibration region (Figure 6A), the strongest features are again the ν_{9a}, ν_{7a}, and ν_{8a} located at 1164, 1214, and 1592 cm^{-1}, respectively. These bands are again located at different positions as compared to the corresponding bands in the normal Raman spectrum. We leave the discussion of this point to the Pd section. Similar to that on Rh, the ν_{8a} also consists of two bands, whose center frequencies are at 1576 and 1592 cm^{-1}, respectively. These can be attributed to the ν_{8a} modes from bridging and atop bound PDI. The majority of the other bands have a similar frequency to those observed on Rh, but the relative intensity is different. For example, the features around 500 cm^{-1} are significantly stronger on Rh than those on Pt. We found that if the Pt surface was soaked in the PDI solution for a significantly shorter time, for example 3 to 4 h as compared to 40 h in Figure 6, these features can be as strong as those bands at around 400 cm^{-1}. This soaking time dependent behavior, which was not observed on other metals, is probably due to the slow structural organization of the PDI layer on Pt. The assignment of other bands is again listed in Table 1.

Although all the bands observed are broadened to some extent as compared to the free molecules, the bandwidth (fwhm) of the majority of the ring vibration modes is less than 30 cm^{-1}. This is sharply in contrast to the ν_{NC} bands which have fwhms in the range of 80 to 110 cm^{-1}. This observation suggests that PDI adsorbs on Pt with one NC group anchoring on the surface and the ring is pendant. To further ensure the end-on adsorption

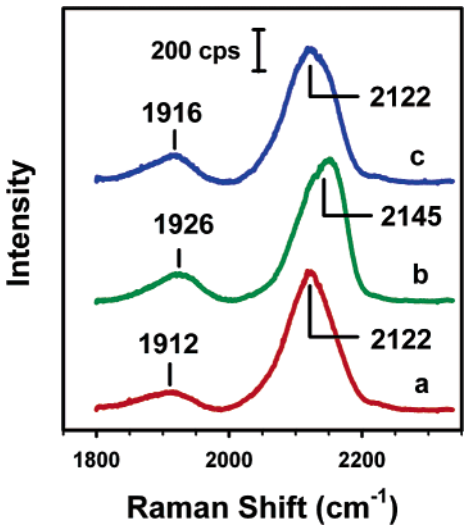

Figure 7. SER spectra of PDI adsorbed on Pt in the N−C stretching region obtained at 0.0 V in (a) 0.1 M $NaClO_4$, (b) CO-saturated 0.1 M $NaClO_4$, and (c) 0.1 M $NaClO_4$ after adsorbed CO was oxidized at +0.8 V. Note the large blueshift of both peaks in the presence of CO.

configuration, CO adsorption was used. Figure 7 shows a set of SER spectra in the N−C and C−O stretching region with and without CO coadsorption, recorded at 0.0 V in 0.1 M $NaClO_4$. Spectrum a was taken on clean Pt after being incubated in 1 mM PDI ethanol solution for 40 h. The spectrum is essentially the same as that shown in Figure 6B. Two bands at 1912 and 2122 cm^{-1} were observed. After the solution was saturated with CO by purging the gas for 5 min, both bands are blueshifted significantly. The 2122 cm^{-1} band upshifts more than 20 wavenumbers, while the 1912 band increases ca. 15 cm^{-1}. The band center frequencies do not change significantly if the solution CO is removed by purging N_2 after CO adsorption. However, after the *adsorbed* CO is removed by oxidation at +0.8 V, the center frequencies essentially move back to the original values. The significant blueshift of the ν_{NC} bands is a result of dynamic dipole coupling, which is commonly observed in CO and NO adlayers.[76−79] The dynamic vibrational dipole coupling is an electrostatic interaction between two adsorbates with parallel vibration dipoles.[76−79] As a result of the coupling, the higher frequency band gains intensity and shifts to a higher wavenumber, while the lower frequency band loses intensity and may not be observable. A more detailed description of the dynamic vibrational dipole coupling can be found in the literature.[76−79]

In the present case, CO adsorption on Pt is known to have two different binding sites. The atop bound CO yields a ν_{CO} at around 2075 cm^{-1} and the bridging bound at 1875 cm^{-1},[49] both are lower than the corresponding values for ν_{NC}. The dipole coupling will then shift both ν_{NC} to higher values, as was observed. It is known that CO adsorbs with C bound to the surface and O pointing away from the surface.[79] The angle between the molecular axis and the surface normal varies, depending on the chemical nature of the metal and CO coverage.[79] The observation of the dipole coupling indicates that PDI adsorbs on Pt through one of the two NC groups with the ring pointing to the solution. Had the PDI adsorbed on Pt with the benzene ring parallel to the surface, there should be no blueshift observed in ν_{NC} because the vibration induced dipole changes in −NC and CO would be orthogonal. The ν_{NC} upshift is not due to the PDI adsorption orientation change upon CO coadsorption, because the ring vibration modes are largely intact after CO adsorption. We did not observe features from the Pt−CO stretching modes, which would be otherwise located at 477 and 390 cm^{-1}, respectively,[49] probably they are too weak and overlap with PDI bands between 400 and 500 cm^{-1}. The edge-on adsorption orientation is in contrast to that reported for Pt films evaporated on Si, on which PDI was believed to adsorb with the benzene ring parallel to the surface, as deduced from the absence of N−C stretching bands in the IR spectrum.[23]

4. PDI Adsorption on Pd. Figure 8 displays a set of SER spectra in both ring vibration (A) and N−C stretching (B) regions obtained on PDI covered Pd in 0.1 M $NaClO_4$. As in the other metals discussed above, the ring vibration region (Figure 8A) does not depend significantly on the applied potential in the range examined, therefore only the spectrum taken at 0.0 V is shown. We begin with the N−C stretching region. Similar to the Pt case, the ν_{NC} region (Figure 8B) contains two bands. Different from Pt, a strong broad (fwhm = 70 cm^{-1}) feature was seen at 1980 to 1990 cm^{-1} depending on the potential, and a weaker but much sharper (fwhm = 30 cm^{-1}) one at around 2122 cm^{-1}, independent of the applied potential. This observation is similar to that reported by Swanson et al.[35] and Murphy et al.[34] using infrared reflection−absorption spectroscopy, except that the lower frequency band is stronger here. The higher frequency is more or equally intense in the IR studies.[34,35] By comparing with the ν_{NC} of trinuclear Pd complexes containing a diisocyanide ligand similar in structure to PDI,[80] Swanson et al. assigned the ν_{NC} at 1980 cm^{-1} to the N−C stretch from the PDI adsorbed on 3-fold hollow sites.[35] The other band at 2122 cm^{-1} was assigned to the N−C stretch of the free NC. The two features observed in Figure 8B can be assigned similarly.

An alternative assignment for the 2122 cm^{-1} band could be the ν_{NC} of the terminal bound PDI, given that the ν_{NC} for monopalladium isocyanide complexes lies between 2139 and 2192 cm^{-1},[81−83] which is close to the higher frequency band in Figure 8B. However, several observations suggest this band assignment is less likely. First, this band is much narrower than the lower frequency partner, suggesting that it is from an NC group not directly interacting with the surface; second, the band is significantly weaker than the lower frequency feature, which can be explained by the NC group away from the surface where the Raman enhancement effect is weaker; third, the ν_{NC} does not vary with the applied potential as the other band does, which can be attributed to the NC group being away from the surface and therefore experiencing a weaker electric field.[57]

To further confirm that the 2122 cm^{-1} feature is from the free NC group, we examined the attachment of gold nanoparticles to the PDI modified Pd. Figure 9 shows a set of SER spectra acquired before (a) and after (b, c) the attachment of Au particles in 0.1 M $NaClO_4$ at 0.0 V. Spectra a were taken after the Pd surface was incubated in 1 mM PDI solution overnight. The spectra largely resemble that shown in Figure 8 at 0.0 V. After the PDI-coated Pd was soaked in a colloidal solution containing 60 nm Au particles for 15 h, the spectrum changes dramatically (Figure 9A). The 1985 cm^{-1} band blueshifts to 1996 cm^{-1} and its intensity increases slightly. Additionally, a new band appears at 2178 cm^{-1}, replacing the 2122 cm^{-1} feature. The new band position is very close to that observed on PDI-covered Au (vide supra) and can be assigned to the ν_{NC} of the NC group bound to the Au nanoparticles. The disappearance of the 2122 cm^{-1} together with the appearance of the 2178 cm^{-1} band indicates the bonding between Au and the originally free NC group. The increase of band intensity arises from a second Raman enhancement effect from the attached gold nanoparticles. The blueshift of the 1985 cm^{-1} band

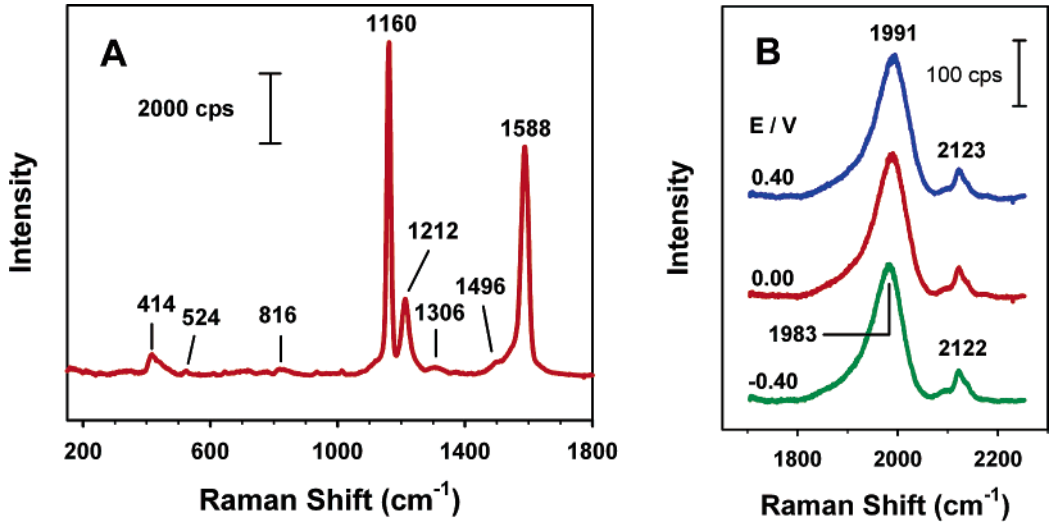

Figure 8. SER spectra obtained on PDI covered Pd electrodes in 0.1 M $NaClO_4$: (A) in the ring vibration region at 0.0 V; (B) in the N−C stretching region at the indicated potentials.

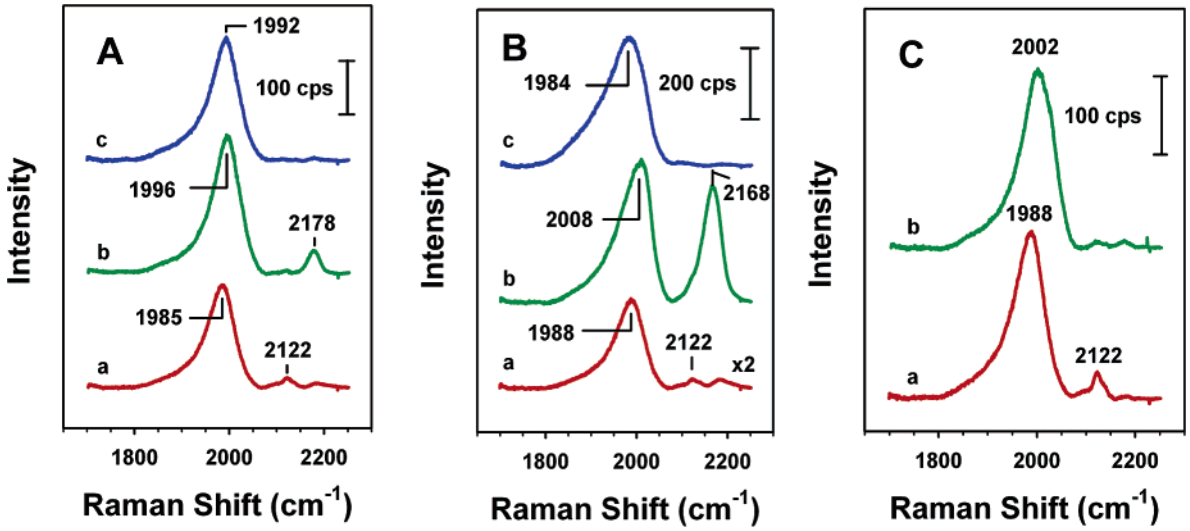

Figure 9. SER spectra obtained on PDI-covered Pd electrodes in 0.1 M $NaClO_4$ in the N−C stretching region at 0.0 V. Spectra were obtained from (a) PDI on Pd, (b) PDI-covered Pd soaked in gold nanoparticles overnight, and (c) after deposition of a monolayer of Pd on the attached Au nanoparticles. Au particle size: (A) 60, (B) 30, and (C) 3 nm.

is an indication of a strong vibration coupling between the two NC groups at each end of the phenyl ring. Similar upshift of ν_{NC} was observed for PDI sandwiched between two gold surfaces in a molecular junction.[29] Interestingly, after a layer of Pd was deposited on the Au nanoparticles by the redox replacement approach (see Experimental Section), the band at 2178 cm^{-1} disappears and the 1996 cm^{-1} band redshifts to 1992 cm^{-1} and becomes broader (Figure 9A). This observation suggests that the attached Au particles can be further modified without being detached from the surface.

We have also examined the attachment of different size Au nanoparticles to the PDI layer (Figure 9B,C). The adsorption of 30 nm Au particles increases the ν_{NC} even more, from 1988 to 2008 cm^{-1}, and its intensity rises nearly four times. In addition, a strong band appears at 2168 cm^{-1}. The band intensity increase is much more significant than the one observed with the 60 nm Au particle, presumably the 30 nm particles aggregate to a larger extent that yields a stronger Raman enhancement effect. Similar to the 60 nm particle adsorption, deposition of a layer of Pd on the 30 nm Au particles triggers a drastic spectral change: the 2178 cm^{-1} band disappears, and the 2008 cm^{-1} band returns to its original value and becomes broader. Interestingly, when 3 nm Au particles were adsorbed, no new band appears probably because the particle is too small to yield significant Raman enhancement for observing the N−C stretching band of isocyanide bound to Au. However, a significant (15 cm^{-1}) blueshift of the 1988 cm^{-1} band as well as the diminishing intensity of the 2122 cm^{-1} feature signify the attachment of Au particles. These results clearly illustrate that PDI adsorbs on Pd edge-on, with one NC group anchoring on the surface and the other pendant. The free NC yields a ν_{NC} at 2122 cm^{-1}, which redshifts from 2128 cm^{-1} of the PDI powder, indicating that the free and bound NC groups are vibrationally coupled.

Murphy et al. observed an additional band at around 2170 cm^{-1} on Pd films, which was assigned to the terminal (atop)-bound PDI.[34] We did not observe a band as strong as they did, but occasionally a weak feature at around 2180 cm^{-1} was observed (Figure 9A,B). This may be from the ν_{NC} of the terminal-bound NC.

By now we have shown that PDI adsorbs exclusively on terminal sites on Au and Ag (data not shown), but on both terminal and high-coordination (bridging and hollow) sites on Pt-group metals. To fully understand this adsorption site

difference requires DFT calculations such as those demonstrated by Koper et al. for CO adsorption.[52] Nevertheless, a qualitative picture can be obtained by analogy to the CO binding as the NC− and CO−metal bonding are similar. As shown beautifully by Koper et al.,[52] the CO adsorption site on different Pt-group metal surfaces is largely determined by the center energy of metal d-band and the filling of the d-orbitals. Higher d-band center energy and d-orbital filling favor π-back-donation and conversely, lower d-band center energy and d-orbital filling result in a stronger σ-donation interaction. The π-back-donation favors adsorbates that bind at high-coordination sites, while the σ-donation prefers the terminal sites. The d-band center energy for Au and Ag is nearly 1 eV lower than that of Pt-group metals;[73,74,84] therefore, it is not surprising that PDI adsorbs exclusively at terminal sites on Au and Ag, but occupies both terminal and high-coordination sites on Pt-group metals. On Pd surfaces, the PDI adsorbs nearly exclusively on 3-fold hollow sites. This adsorption site preference may be due to the higher d-orbital filling as compared to Rh, which has a similar d-band energy, and the higher d-band center as compared to Pt.

We now turn to the ring vibration region. Similar to other metals discussed above, the most intense are three bands at 1160, 1212, and 1588 cm^{-1}, assigned to ν_{9a}, ν_{7a}, and ν_{8a}, respectively. As we have seen on other metals, the ν_{9a} and ν_{8a} decreases, while the ν_{7a} increases significantly from the corresponding values for the free PDI. This may be understood in terms of PDI−metal bonding. The ν_{8a} is one of the C−C stretching modes. The σ-donation will weaken the C−C bond parallel to the molecular axis (see Supporting Information , Figure 4S). This may be the reason for the redshift of the ν_{8a} upon adsorption on Au. Similarly for the ν_{9a} mode, which is a C−H in-plane bend coupled to the ring breathing, the weakening of the C−C bond will also soften the C−H bending. The π-back-donation may soften the C−C stretch even more because it contributes to the orbital that is largely C−C antibonding (Figure 4S). Consequently, the more back-donation, the lower the frequency. Compared to other metals examined above, the ν_{9a} and especially the ν_{8a} have the lowest frequency on Pd (Table 1), which may be related to the mainly hollow site binding on Pd, i.e., more π-back-donation to the attached NC group. In contrast to ν_{9a} and ν_{8a}, however, ν_{7a} is blueshifted more than 10 cm^{-1} upon adsorption. Although a systematic change with the degree of π-back-donation is not as clear-cut as the former two modes, the blueshift is consistently observed on different metals (Table 1). This can again be understood in terms of the PDI−metal bonding. The ν_{7a} is a C−NC stretch mainly involving the nitrogen in the NC group and the ring carbon bound to the NC. Both the σ-donation and π-back-donation would strengthen the C−NC bond (Figure 4S), therefore upon adsorption ν_{7a} is upshifted. The frequency shift is larger on Pt-group metals than on Au, which may be a result of significant contributions to the M−CN bond from both σ-donation and π-back-donation, as compared to mainly σ-donation on Au.

Another noticeable spectral difference between Pd and other metals is the relative intensity of the bands at 416 and 822 cm^{-1}, which are assigned to the ν_{16a} and ν_1 modes, respectively. On all of the other metals, the 822 cm^{-1} band is weaker than its neighbor at 840 cm^{-1}, but on Pd the former is stronger. Similarly, on Pd the ν_{16a} is the strongest among the features around 400 cm^{-1}. This relative band intensity change is also likely a result of hollow site binding, as compared to other metals where the atop site binding is dominant. There are other much weaker bands discernible in the spectrum. The tentative assignment of these bands is listed in Table 1. The fwhm of most of the observed bands is smaller than 30 cm^{-1}, which again supports the edge-on adsorption of PDI.

IV. Conclusions

In summary, we have shown surface-enhanced Raman spectra of PDI adsorbed on Au and Pt-group transition metals in the electrochemical environment. From these spectroscopic results, the PDI adsorption orientation and sites can be deduced. On all of the metal surfaces examined here, PDI adsorbs with only one isocyanide group attached to the surfaces and the benzene ring pointing away from the surface. The adsorption sites, inferred mainly from the comparison of the NC stretching frequency to that of the corresponding inorganic complexes, differ significantly among different metals. On Au, PDI adsorbs only to atop sites. On Rh and Pt, both atop and bridging bound PDIs were observed, but the former adsorption is predominant as suggested by its more intense SER band. On Pd, PDI adsorbs to 3-fold hollow sites most favorably, though terminal bound PDI was occasionally observed. This binding site preference is likely due to the difference in the d-band center energy and d-orbital filling of the metals. Corresponding to the different binding sites, some of the ring vibration modes are also metal dependent, most notably the C−C stretch, ν_{8a}. The softening of ν_{8a} is likely because both the σ-donation and π-back-donation weaken the C−C bond. The finding that the isocyanide binding site is metal dependent should have an implication on the molecular electronic development. The NC group bound to different binding sites will likely influence the electron transport properties at the molecule−metal junction,[34] which has yet to be explored systematically. We have recently initiated simultaneous surface-enhanced Raman and electrical conductivity measurements of PDI sandwiched between two Au electrodes.[29] It will be interesting to use this approach to examine the effects of metals on the conductivity as well as the correlation between binding site and conductivity.

Acknowledgment. This work is supported in part by Miami University through startup funds and by the National Science Foundation under ECS-0403669. S.G. and M.H. were supported by the Miami University Undergraduate Summer Scholar program. We thank Mr. Shengqian Ma for his assistance in obtaining the IR spectrum of PDI powder and the instrument laboratory of Miami University for the modification of the thermal evaporator used in the Au thin film preparation.

Supporting Information Available: An IR spectrum of PDI powder, a set of SER spectra showing the oxidation of PDI on Au, a ν_{NC}−applied potential plot for PDI on Rh, and a cartoon of molecular orbitals involved in PDI−metal bonding. This material is available free of charge via the Internet at http://pubs.acs.org.

References and Notes

(1) Chen, J.; Reed, M. A. *Chem. Phys.* **2002**, *281*, 127.
(2) Tour, J. M. *Acc. Chem. Res.* **2000**, *33*, 791.
(3) Ulman, A. *An introduction to ultrathin organic films*: *from Langmuir−Blodgett to self-assembly*; Academic Press: Boston, MA, 1991.
(4) Ulman, A. *Chem. Rev.* **1996**, *96*, 1533.
(5) McCreery, R. L. *Chem. Mater.* **2004**, *16*, 4477.
(6) Seminario, J. M.; De la Cruz, C. E.; Derosa, P. A. *J. Am. Chem. Soc.* **2001**, *123*, 5616.
(7) Beebe, J. M.; Engelkes, V. B.; Miller, L. L.; Frisbie, C. D. *J. Am. Chem. Soc.* **2002**, *124*, 11268.
(8) Chen, J.; Calvet, L. C.; Reed, M. A.; Carr, D. W.; Grubisha, D. S.; Bennett, D. W. *Chem. Phys. Lett.* **1999**, *313*, 741.
(9) Hahn, F. E. *Angew. Chem.*; *Int. Ed.* **1993**, *32*, 650.

(10) Malatesta, L.; Bonati, F. *Isocyanide complexes of metals*; John Wiley & Sons: New York, 1969.
(11) Singleton, E.; Oosthuizen, H. E. In *Advances in Organometallic Chemistry*; Stone, F. G. A., West, R., Eds.; Academic Press: New York, 1983; Vol. 22, pp 209−310.
(12) Treichel, P. M. In *Advances in Organometallic Chemistry*; Stone, F. G. A., West, R., Eds.; Academic Press: New York, 1973; Vol. II, pp 21−86.
(13) Friend, C. M.; Muetterties, E. L.; Gland, J. L. *J. Phys. Chem.* **1981**, *85*, 3256.
(14) Semancik, S.; Haller, G. L.; Yates, J. T. *J. Chem. Phys.* **1983**, *78*, 6970.
(15) Avery, N. R.; Matheson, T. W. *Surf. Sci.* **1984**, *143*, 110.
(16) Kang, D.-H.; Trenary, M. *J. Phys. Chem. B* **2002**, *106*, 5710.
(17) Murphy, K.; Azad, S.; Bennett, D. W.; Tysoe, W. T. *Surf. Sci.* **2000**, *467*, 1.
(18) Ontko, A. C.; Angelici, R. J. *Langmuir* **1998**, *14*, 1684.
(19) Ontko, A. C.; Angelici, R. J. *Langmuir* **1998**, *14*, 3071.
(20) Robertson, M. J.; Angelici, R. J. *Langmuir* **1994**, *10*, 1488.
(21) Shih, K.-C.; Angelici, R. J. *Langmuir* **1995**, *11*, 2539.
(22) Henderson, J. I.; Feng, S.; Bein, T.; Kubiak, C. P. *Langmuir* **2000**, *16*, 6183.
(23) Pranger, L.; Tannenbaum, R. *J. Colloid Interface Sci.* **2005**, *292*, 71.
(24) Pranger, L.; Goldstein, A.; Tannenbaum, R. *Langmuir* **2005**, *21*, 5396.
(25) Han, H. S.; Han, S. W.; Joo, S. W.; Kim, K. *Langmuir* **1999**, *15*, 6868.
(26) Joo, S. W.; Kim, W. J.; Yoon, W. S.; Choi, I. S. *J. Raman Spectrosc.* **2003**, *34*, 271.
(27) Joo, S. W.; Kim, W. J.; Yun, W. S.; Hwang, S.; Choi, I. S. *Appl. Spectrosc.* **2004**, *58*, 218.
(28) Kim, H. S.; Lee, S. J.; Kim, N. H.; Yoon, J. K.; Park, H. K.; Kim, K. *Langmuir* **2003**, *19*, 6701.
(29) Jaiswal, A.; Tavakoli, K. G.; Zou, S. *Anal. Chem.* **2006**, *78*, 120.
(30) Hickman, J. J.; Laibinis, P. E.; Auerbach, D. I.; Zou, C.; Gardner, T. J.; Whitesides, G. M.; Wrighton, M. S. *Langmuir* **1992**, *8*, 357.
(31) Hickman, J. J.; Zou, C. F.; Ofer, D.; Harvey, P. D.; Wrighton, M. S.; Laibinis, P. E.; Bain, C. D.; Whitesides, G. M. *J. Am. Chem. Soc.* **1989**, *111*, 7271.
(32) Lin, S.; McCarley, R. L. *Langmuir* **1999**, *15*, 151.
(33) Horswell, S. L.; Kiely, C. J.; O'Neil, I. A.; Schiffrin, D. J. *J. Am. Chem. Soc.* **1999**, *121*, 5573.
(34) Murphy, K. L.; Tysoe, W. T.; Bennett, D. W. *Langmuir* **2004**, *20*, 1732.
(35) Swanson, S. A.; McClain, R.; Lovejoy, K. S.; Alamdari, N. B.; Hamilton, J. S.; Scott, J. C. *Langmuir* **2005**, *21*, 5034.
(36) Stapleton, J. J.; Daniel, T. A.; Uppili, S.; Cabarcos, O. M.; Naciri, J.; Shashidhar, R.; Allara, D. L. *Langmuir* **2005**, *21*, 11061.
(37) Tian, Z. Q.; Ren, B. *Annu. Rev. Phys. Chem.* **2004**, *55*, 197.
(38) Weaver, M. J.; Zou, S. Z. In *Interfacial Electrochemistry*; Wieckowski, A., Ed.; Marcel Dekker: New York, 1999; pp 301−316.
(39) Brown, K. R.; Walter, D. G.; Natan, M. J. *Chem. Mater.* **2000**, *12*, 306.
(40) Grabar, K. C.; Freeman, R. G.; Hommer, M. B.; Natan, M. J. *Anal. Chem.* **1995**, *67*, 735.
(41) Semaltianos, N. G.; Wilson, E. G. *Thin Solid Films* **2000**, *366*, 111.
(42) Derose, J. A.; Lampner, D. B.; Lindsay, S. M.; Tao, N. J. *J. Vac. Sci. Technol. A* **1993**, *11*, 776.
(43) Hwang, J.; Dubson, M. A. *J. Appl. Phys.* **1992**, *72*, 1852.
(44) Gao, P.; Gosztola, D.; Leung, L. W. H.; Weaver, M. J. *J. Electroanal. Chem.* **1987**, *233*, 211.
(45) Weaver, M. J.; Zou, S. Z.; Chan, H. Y. H. *Anal. Chem.* **2000**, *72*, 38A.
(46) Park, S.; Yang, P. X.; Corredor, P.; Weaver, M. J. *J. Am. Chem. Soc.* **2002**, *124*, 2428.
(47) Mrozek, M. F.; Xie, Y.; Weaver, M. J. *Anal. Chem.* **2001**, *73*, 5953.
(48) Brankovic, S. R.; Wang, J. X.; Adzic, R. R. *Surf. Sci.* **2001**, *474*, L173.
(49) Zou, S. Z.; Weaver, M. J. *Anal. Chem.* **1998**, *70*, 2387.
(50) Zou, S. Z.; Williams, C. T.; Chen, E. K. Y.; Weaver, M. J. *J. Am. Chem. Soc.* **1998**, *120*, 3811.
(51) Irwin, M. J.; Jia, G. C.; Payne, N. C.; Puddephatt, R. J. *Organometallics* **1996**, *15*, 51.
(52) Koper, M. T. M.; van Santen, R. A.; Wasileski, S. A.; Weaver, M. J. *J. Chem. Phys.* **2000**, *113*, 4392.
(53) Blyholder, G. *J. Phys. Chem.* **1964**, *68*, 2772.
(54) Zou, S. Z.; Weaver, M. J. *J. Phys. Chem.* **1996**, *100*, 4237.
(55) Lambert, D. K. *J. Chem. Phys.* **1988**, *89*, 3847.
(56) Korzeniewski, C.; Pons, S.; Schmidt, P. P.; Severson, M. W. *J. Chem. Phys.* **1986**, *85*, 4153.
(57) Oklejas, V.; Sjostrom, C.; Harris, J. M. *J. Am. Chem. Soc.* **2002**, *124*, 2408.
(58) Horswell, S. L.; O'Neil, I. A.; Schiffrin, D. J. *J. Phys. Chem. B* **2003**, *107*, 4844.
(59) Frisch, M. J. et al. *Gaussian 03*, Revision B.04; Gaussian, Inc.: Pittsburgh, PA, 2003.
(60) Varsanyi, G. *Assignments for vibrational spectra of seven hundred benzene derivatives*; John Wiley & Sons: New York, 1974.
(61) Halls, M. D.; Velkovski, J.; Schlegel, H. B. *Theor. Chem. Acc.* **2001**, *105*, 413.
(62) Palafox, M. A. *J. Phys. Chem. A* **1999**, *103*, 11366.
(63) Scott, A. P.; Radom, L. *J. Phys. Chem.* **1996**, *100*, 16502.
(64) Creighton, J. A. In *Spectroscopy of Surfaces*; Clark, R. J. H., Hester, R. E., Eds.; John Wiley & Sons: New York, 1988; Vol. 16, pp 37−90.
(65) Moskovits, M. *Rev. Mod. Phys.* **1985**, *57*, 783.
(66) Ansell, M. A.; Cogan, E. B.; Page, C. J. *Langmuir* **2000**, *16*, 1172.
(67) Henderson, J. I.; Feng, S.; Ferrence, G. M.; Bein, T.; Kubiak, C. P. *Inorg. Chim. Acta* **1996**, *242*, 115.
(68) Huc, V.; Bourgoin, J.-P.; Bureau, C.; Valin, F.; Zalczer, G.; Palacin, S. *J. Phys. Chem. B* **1999**, *103*, 10489.
(69) Musick, M. D.; Keating, C. D.; Lyon, L. A.; Botsko, S. L.; Pena, D. J.; Holliway, W. D.; McEvoy, T. M.; Richardson, J. N.; Natan, M. J. *Chem. Mater.* **2000**, *12*, 2869.
(70) Vicente, J.; Gil-Rubio, J.; Guerrero-Leal, J.; Bautista, D. *Organometallics* **2005**, *24*, 5634.
(71) Winzenburg, M. L.; Kargol, J. A.; Angelici, R. J. *J. Organomet. Chem.* **1983**, *249*, 415.
(72) Efraty, A.; Feinstein, I.; Frolow, F.; Wackerle, L. *J. Am. Chem. Soc.* **1980**, *102*, 6341.
(73) Hammer, B.; Norskov, J. K. In *Advances in Catalysis*: *Impact of surface science on catalysis*; Gates, B. C., Knozinger, H., Eds.; Academic Press: San Diego, CA, 2000; Vol. 45, pp 71−129.
(74) Skriver, H. L.; Rosengaard, N. M. *Phys. Rev. B* **1992**, *46*, 7157.
(75) Bradford, A. M.; Kristof, E.; Rashidi, M.; Yang, D. S.; Payne, N. C.; Puddephatt, R. J. *Inorg. Chem.* **1994**, *33*, 2355.
(76) Tang, C.; Zou, S. Z.; Severson, M. W.; Weaver, M. J. *J. Phys. Chem. B* **1998**, *102*, 8546.
(77) Weaver, M. J.; Tang, C.; Zou, S. Z.; Severson, M. W. *J. Chem. Phys.* **1998**, *109*, 4135.
(78) Ryberg, R. *Adv. Chem. Phys.* **1989**, *76*, 1.
(79) Hollins, P.; Pritchard, J. *Prog. Surf. Sci.* **1985**, *19*, 275.
(80) Rashidi, M.; Kristof, E.; Vittal, J. J.; Puddephatt, R. J. *Inorg. Chem.* **1994**, *33*, 1497.
(81) Tanase, T.; Ukaji, H.; Yamamoto, Y. *J. Chem. Soc., Dalton Trans.* **1996**, 3059.
(82) Tanase, T.; Ohizumi, T.; Kobayashi, K.; Yamamoto, Y. *Organometallics* **1996**, *15*, 3404.
(83) Rashidi, M.; Vittal, J. J.; Puddephatt, R. J. *J. Chem. Soc., Dalton Trans.* **1994**, 1283.
(84) Weaver, M. J.; Zou, S. Z.; Tang, C. *J. Chem. Phys.* **1999**, *111*, 368.